Recombination effects during expansion into vacuum in laser produced Sn plasma

Russell A. Burdt,[a] Yoshifumi Ueno, Yezheng Tao, Sam Yuspeh, Mark S. Tillack, and Farrokh Najmabadi

Center for Energy Research, University of California San Diego, 9500 Gilman Drive, La Jolla, California 92093, USA

(Received 10 June 2010; accepted 12 July 2010; published online 30 July 2010)

The distance over which the charge state distribution evolves during the expansion of laser produced Sn plasma in vacuum is investigated experimentally. This distance is found to be less than 6 cm with a planar target irradiated by a 1.064 μm laser at 8.3×10^{11} W/cm^2 but greater than 60 cm when a 10.6 μm laser at 2.5×10^{10} W/cm^2 is used. The difference is attributed to the laser wavelength dependence of the coronal electron density and the subsequent recombination processes during expansion. Important implications to the extreme ultraviolet x-ray source application are discussed specifically. © *2010 American Institute of Physics*. [doi:10.1063/1.3473817]

High charge state ions can be measured meters away in vacuum from the interaction of a solid target with focused laser radiation at low[1] ($<10^{12}$ W/cm^2), high[2] ($\sim10^{15}$ W/cm^2), and relativistic[3] ($\sim10^{19}$ W/cm^2) intensities. Complete recombination is prevented by fast plasma expansion to a sufficiently rarefied state where recombination processes become negligible. The distance from the target surface over which the charge state distribution evolves before freezing for subsequent expansion, hereafter referred to as the critical distance, is therefore, significantly affected by the laser parameters determining the initial recombination rates, in particular the laser wavelength.[1,4]

Charge state freezing in laser produced plasma (LPP) has important implications for several applications. In a laser ion source, the high charge state ions are useful for extraction and injection into accelerators.[2] Alternatively, in the extreme ultraviolet (EUV) x-ray source application the high charge state ions damage downstream optical components. Tin plasma produced by both gas and solid-state lasers is utilized as an efficient source of EUV radiation at 13.5 nm, the next step down in wavelength of lithography light sources enabling ever-decreasing features on integrated circuits.[5] The EUV radiation emitted by the plasma is collected and focused with a large and expensive x-ray optic surrounding the plasma. A significant research effort has focused on ion mitigation methods designed to minimize damage to the EUV x-ray optic.[6] However, few efforts characterize the evolution of the ion populations during expansion in vacuum, which would both advance the development of ion mitigation methods for a commercial system and provide a better understanding of the relevant physics. Here we study experimentally the critical distance for Sn plasma produced by neodymium-doped yttrium aluminum garnet (Nd:YAG) and CO_2 lasers, along with measurements of the angular distribution and charge state distribution of emitted ions.

The critical distance is measured by scanning a faraday cup along the path of plasma expansion; a diagram of the experimental arrangement is shown in Fig. 1. The faraday cup is biased to measure the time-resolved ion current from the LPP, and the ion current is time-integrated to give the total ionic charge collected by the faraday cup at the distance L from the target, $Q_i(L)$. This quantity will be a fraction of the total ionic charge emitted into 2π sr as measured at the distance L, Q_{i0}, related by

$$Q_{i0} = Q_i(\Omega_{eff}/2\pi), \tag{1}$$

where Ω_{eff} is the effective solid angle of the faraday cup,

$$\Omega_{eff} = \int_0^{2\pi}\int_0^{\Theta} \cos^p(\theta+\alpha)\sin\theta d\theta d\phi, \tag{2}$$

and the integration is over the circular aperture of the faraday cup, i.e., $\Theta=\tan^{-1}(D/2L)$. The normalized angular distribution of emitted ions (symmetric about the laser axis) is represented by $\cos^p(\theta+\alpha)$, which is an empirical fit to experimental data.[7] When the angular distribution is isotropic ($p=0$), the usual expression for solid angle is recovered. If the calculated quantity Q_{i0} is constant within the error bars as the faraday cup is scanned away from the target, this implies the charge state distribution has stopped evolving in that interval and will be frozen for subsequent expansion. However, if Q_{i0} is decreasing as the faraday cup is scanned away from the target, this implies the ion populations are recombining to lower charge states within that interval.

Similar experiments and analyses have been used to demonstrate a decaying charge state distribution up to 15 cm

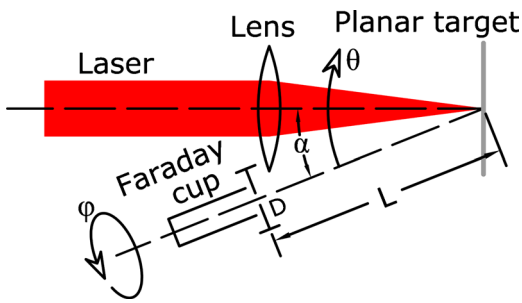

FIG. 1. (Color online) Experimental arrangement for measurement of the critical distance. A focused laser irradiates a planar target at normal incidence. A faraday cup with aperture diameter D is installed at an angle α to the target normal and can be translated distances L along the path of plasma expansion. A spherical coordinate system with zenith angle θ and azimuthal angle φ with respect to the faraday cup translation axis is superimposed.

[a]Electronic mail: russellburdt@yahoo.com.

TABLE I. Laser parameters used in the experiments. Our Nd:YAG laser is a Continuum Surelite II-10, and our CO_2 laser is custom-built and described elsewhere.[9] The focusing lens in each experiment is planoconvex with focal length f given in the table. At each laser wavelength, the focal diameter was measured directly with an appropriate imaging lens and camera.

Wavelength (μm)	Full width at half maximum pulse duration (ns)	Pulse energy (mJ)	$(1/e^2)$ focal diameter (μm)	f (cm)	Resultant laser intensity (W/cm^2)
1.064	7	165	60	30	8.3×10^{11}
10.6	35	50	85	6.4	2.5×10^{10}

away from a Cu target irradiated by a low intensity XeCl laser,[8] and a frozen-in charge state distribution after 82 cm of expansion from various high-Z targets irradiated by a high-intensity iodine laser,[2] both to support the laser ion source application. The topic of charge state freezing in LPP has been treated theoretically[4] as well, where a scaling law for the critical distance, L_{CR}, was derived,

$$L_{CR} \propto (T_e^{13/12} v_i^{14/6} \tau_L^{13/6})/(n_c^{8/18} d_S^{8/6}). \quad (3)$$

Typical parameters relevant to the EUV x-ray source application are electron temperature, $T_e \approx 30-40$ eV, ion velocity, $v_i \approx 2\times10^6$ cm/s, and laser focal diameter, $d_S \approx 100$ μm, all irrespective of laser wavelength. The critical electron density, n_c, is laser wavelength-dependent and for Nd:YAG LPP is $n_c \approx 10^{21}$ cm^{-3}, and for CO_2 LPP is $n_c \approx 10^{19}$ cm^{-3}. The pulse duration, τ_L, is generally longer for CO_2 lasers as compared to Nd:YAG lasers. It was estimated by Roudskoy[4] that at moderate laser intensities ($<10^{15}/\lambda^2$ $W/cm^2/\mu m^2$, where λ is the laser wavelength), L_{CR} would be on the order of centimeters for $\lambda \approx 1$ μm but could reach up to meters for $\lambda \approx 10$ μm.

The critical distance was measured in the parameter space summarized in Table I. A photodiode and laser energy monitor were installed in the optical path in both experiments to ensure repeatable irradiation conditions for each laser pulse. The targets were high-purity (>3N) Sn slabs which were translated in the focal plane before each shot to provide a fresh surface, and all experiments were conducted in vacuum below 3×10^{-6} torr so charge exchange with the ambient was negligible.

For the calculation of effective solid angle [Eq. (2)], the functional form of the angular distribution of emitted ions must be known, specifically the exponent p in the fitting function $\cos^p(\theta+\alpha)$. Tanaka *et al.*[7] have measured p for Nd:YAG LPP at intensities on the order of 10^{11} W/cm^2 to be approximately 2, in agreement with data from other authors in similar parameter space. The angular distribution of emitted ions from the CO_2 LPP was measured directly, as prior data in our parameter space was not available. Four identical faraday cups were installed in a vacuum chamber, each 105 cm from the target, at angles of 27.0°, 37.3°, 52.9°, and 68.4° with respect to the target normal. Target and CO_2 laser parameters were identical for all experiments. Typical signals recorded simultaneously from all four faraday cups are in Fig. 2(a), and a polar plot of mean ion energy is in Fig. 2(b). A function of the form $\lambda_1 \cos^p \theta+\lambda_2$ was fit in a least-squares sense to the data, and p=1.75 was obtained.

The results of the critical distance experiments at both laser wavelengths are in Fig. 3. Using the Nd:YAG laser, the faraday cup was scanned from 55 to 160 mm on a translation stage inside the vacuum chamber and over this interval Q_{i0} was constant, within the possible error, indicating the critical distance to be less than 55 mm. The exact critical distance could not be measured as the faraday cup could not be scanned any closer to the target due to power limitations and eventually breakdown within the faraday cup. The laser intensity used in this experiment (8.3×10^{11} W/cm^2) is a few times higher than the optimal laser intensity at this wavelength for the EUV x-ray source application ($\approx 2\times10^{11}$ W/cm^2),[1] however, the scaling law for critical distance [Eq. (3)] predicts at lower laser intensities (lower electron temperature) the critical distance will be even shorter.[4]

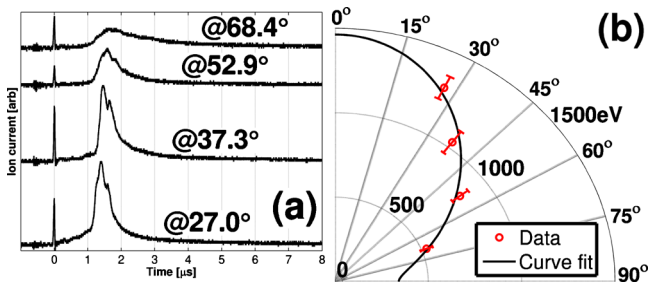

FIG. 2. (Color online) Typical signals recorded simultaneously from each of the four faraday cups are shown in (a), offset from each other but with the same vertical scale. A polar plot of mean ion energy and a least-squares curve fit is shown in (b); 0° is the target normal. The mean ion energy is calculated as $\langle E\rangle=(M/2)(d/t)^2$, where M is the ion mass (118.71 amu for Sn), d is distance from each faraday cup to the target (105 cm), and $\langle t\rangle = \int_0^\infty t\times v(t)dt / \int_0^\infty v(t)dt$, where $v(t)$ is the measured voltage from the faraday cup as a function of time. The calculated mean ion energies in (b) were averaged from 20 shots.

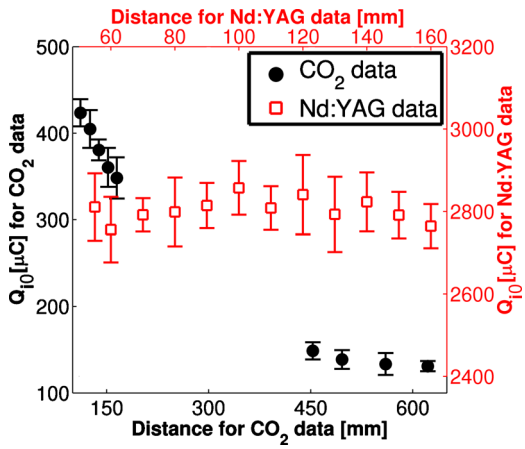

FIG. 3. (Color online) Q_{i0} as a function of distance from the faraday cup to the target. Solid circles represent data using the CO_2 laser; open squares represent data using the Nd:YAG laser. Each data point is the average of least 15 shots. For the Nd:YAG data Q_{i0} is constant within the error bars implying the critical distance is less than 55 mm. For the CO_2 data Q_{i0} is decaying over both spatial intervals investigated, implying the critical distance is greater than 622 mm.

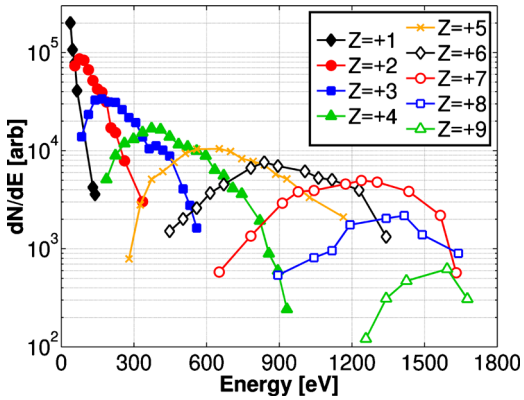

FIG. 4. (Color online) Charge-state resolved ion energy distribution measured at a distance of 100 cm from a Sn target irradiated by a CO_2 laser with parameters described in Table I.

As a result of the short critical distance, previous measurements of the charge state distribution, which are recorded at distances close to 100 cm from the target due to diagnostic limitations, should represent the charge state distribution 10 cm from the target, the distance where the x-ray collector optic would be located in an EUV x-ray source.[1,10]

Using the CO_2 laser, Q_{i0} was measured over two spatial intervals. From 112 to 165 mm a faraday cup mounted on a translation stage inside the vacuum chamber was used, and from 453 to 622 mm a flange-mounted faraday cup on a variety of vacuum extensions mounted on the chamber wall was used. The physical differences in the two faraday cups (aperture size, grid transparency) were taken into account in comparing the data quantitatively. The faraday cup could not be scanned any closer to the target because it was blocked by the short focal length lens in the vacuum chamber, and other devices on our optical table blocked the faraday cup from extending farther distances. Over both spatial intervals Q_{i0} has a negative slope, indicating the critical distance to be greater than 622 mm, in agreement with the theoretical prediction by Roudskoy[4] that L_{CR} should be on the order of meters for $\lambda \approx 10$ μm. About four to five times less charge was emitted from the CO_2 LPP as compared to the Nd:YAG LPP at the same distance, which is consistent with previous studies and due to decreased mass ablation at the longer laser wavelength.[5,11]

Due to the long critical distance of the CO_2 LPP, measurements of the charge state distribution at distances of 100 cm from the target[1] will not represent the actual charge state distribution at distances closer to the target; the average ion charge state will be underestimated. Our diagnostic for measuring the charge state distribution has been discussed elsewhere,[1,5] and was used here to measure the distribution for the CO_2 LPP at a distance 100 cm from the target; results are in Fig. 4. The average ion charge state can be calculated from the data in Fig. 4 and is 3 ± 1; the error is due to insufficient resolution of the peak of the Z=+1 ion energy distribution. The average charge state at the target surface cannot be inferred exactly from a combination of the charge state distribution data (Fig. 4) and critical distance measurements (Fig. 3), however, it can be estimated as approximately five times the value measured 100 cm from the target by extrapolating the data of Fig. 3 with a least-squares curve fit. An average charge state of approximately 15 near the target surface is estimated from the ion properties measured here, which is in agreement with detailed atomic modeling of Sn plasma by Sasaki *et al.*[12]

The greater than order of magnitude difference in critical distance for the two plasmas studied here is due to the effects of laser wavelength on the initial recombination rates. As mentioned previously, the ion charge state distribution becomes frozen for subsequent expansion only after all recombination processes are negligible. The dominant recombination mechanism during expansion, three-body recombination, will only become negligible if the adiabatic cooling of electron temperature is slowed by a release of energy to free electrons, which is provided by a release of residual energy in each act of three-body recombination, as discussed in detail in Rumsby and Paul.[13] The critical distance should be shorter at the lower laser wavelength because the higher initial electron density of the Nd:YAG LPP leads to a higher initial three-body recombination rate, and thus more residual energy is released to free electrons in three-body recombination. The same qualitative trend is predicted by the scaling law for L_{CR} [Eq. (3)], which is originally derived by balancing the energy released in each act of three-body recombination with the specific energy loss due to hydrodynamic expansion.[4] The fact that laser intensities were different in the two experiments does not discredit the result, the difference in critical distance would be even more pronounced at equal laser intensities according to the scaling law for L_{CR}.

An additional implication of the critical distance is that electrostatic and magnetostatic fields should be more effective at mitigating ions from Sn plasma produced by longer laser wavelengths, in which the plasma retains its high charge state ions over long distances from the target. Published experimental data on the effectiveness of magnetic field mitigation as a function of laser wavelength is not conclusive at this time as to which wavelength is best.[14,15] More detailed experimental comparisons shoud be carried out to clarify this point.

[1]R. A. Burdt, Y. Tao, M. S. Tillack, S. Yuspeh, N. M. Shaikh, E. Flaxer, and F. Najmabadi, J. Appl. Phys. **107**, 043303 (2010).
[2]J. Krása, L. Laska, K. Rohlena, M. Pfeifer, J. Skala, B. Kralikova, P. Straka, E. Woryna, and J. Wolowski, Appl. Phys. Lett. **75**, 2539 (1999).
[3]E. L. Clark, K. Krushelnick, M. Zepf, F. N. Beg, M. Tatarakis, A. Machacek, M. I. K. Santala, I. Watts, P. A. Norreys, and A. E. Dangor, Phys. Rev. Lett. **85**, 1654 (2000).
[4]I. V. Roudskoy, Laser Part. Beams **14**, 369 (1996).
[5]R. A. Burdt, S. Yuspeh, K. L. Sequoia, Y. Tao, M. S. Tillack, and F. Najmabadi, J. Appl. Phys. **106**, 033310 (2009).
[6]Y. Tao and M. S. Tillack, Appl. Phys. Lett. **89**, 111502 (2006).
[7]H. Tanaka, A. Matsumoto, K. Akinaga, A. Takahashi, and T. Okada, Appl. Phys. Lett. **87**, 041503 (2005).
[8]A. Lorusso, J. Krasa, K. Rohlena, V. Nassisi, F. Belloni, and D. Doria, Appl. Phys. Lett. **86**, 081501 (2005).
[9]Y. Tao, M. S. Tillack, N. Amin, R. A. Burdt, S. Yuspeh, N. M. Shaikh, and F. Najmbadi, Rev. Sci. Instrum. **80**, 123503 (2009).
[10]S. Fujioka, H. Nishimura, K. Nishihara, M. Murakami, Y. Kang, Q. Gu, K. Nagai, T. Norimatsu, N. Miyanaga, Y. Izawa, K. Mima, Y. Shimada, A. Sunahara, and H. Furukawa, Appl. Phys. Lett. **87**, 241503 (2005).
[11]A. Takahashi, D. Nakamura, K. Tamaru, T. Akiyama, and T. Okada, Appl. Phys. B: Lasers Opt. **92**, 73 (2008).
[12]A. Sasaki, A. Sunahara, K. Nishihara, T. Nishikawa, F. Koike, and H. Tanuma, J. Phys.: Conf. Ser. **112**, 042062 (2008).
[13]P. T. Rumsby and J. W. M. Paul, Plasma Phys. **16**, 247 (1974).
[14]S. S. Harilal, B. O'Shay, Y. Tao, and M. S. Tillack, Appl. Phys. B: Lasers Opt. **86**, 547 (2007).
[15]Y. Ueno, G. Soumagne, A. Sumitani, A. Endo, T. Higashiguchi, and N. Yugami, Appl. Phys. Lett. **92**, 211503 (2008).